THE BILE ACID TUDCA INCREASES GLUCOSE-INDUCED INSULIN SECRETION VIA THE cAMP/PKA PATHWAY IN PANCREATIC BETA CELLS

Jean Franciesco Vettorazzi[1,4], Rosane Aparecida Ribeiro[2], Patricia Cristine Borck[1], Renato Chaves Souto Branco[1], Sergi Soriano[3], Beatriz Merino[4], Antônio Carlos Boschero[1], Angel Nadal[4], Ivan Quesada[4a], and Everardo Magalhães Carneiro[1a*]

[1]Department of Structural and Functional Biology, Institute of Biology, University of Campinas (UNICAMP), 13083-970 Campinas, SP, Brazil

[2]Integrated Laboratory of Morfology, Centre for Ecology and Socio-Environmental – NUPEM, Federal University of Rio de Janeiro (UFRJ), Macaé, Rio de Janeiro, Brazil

[3]Department of Physiology, Genetics and Microbiology, University of Alicante, 03080 Alicante, Spain

[4]Institute of Bioengineering and the Biomedical Research Center in Diabetes and Associated Metabolic Disorders (CIBERDEM), Miguel Hernández University, 03202, Elche, Spain

[a]These authors equally contributed to this work.

*__Corresponding author:__ Everardo Magalhães Carneiro, Department of Structural and Functional Biology, Institute of Biology, University of Campinas (UNICAMP), Monteiro Lobato Street, 13083-970, Campinas, SP, Brazil. Phone: +55 1935216203. Email: emc@unicamp.br.

Abbreviations:

6E-CDCA: 6-Ethyl-chedeoxycholic acid

ADP: Adenosine diphosphate

AKT or PTB: Protein kinase B

ATP: Adenosine triphosphate

AUC: Area under curve

BSA: Bovine serum albumin

cAMP: Cyclic adenosine monophosphate

CREB: cAMP response element-binding protein

DZX: Diazoxide

FXR: Farnesoid X Receptor

GAPDH: Glyceraldehyde 3-phosphate dehydrogenase

GLP-1: Glucagon-like peptide 1

GLUT-2: Glucose transporter 2

GSIS: Glucose-stimulated insulin secretion

H89: Protein kinase A inhibitor

INT-777: 6-Alpha-ethyl-23(*S*)-methyl-cholic acid

K_{ATP}: ATP-sensitive K^+ channel

KLF 11: Kruppel-like factor 11

NAD(P)H: Nicotinamide adenine dinucleotide phosphate

NF449: Gsα-subunit G protein antagonist

OA: Oleanolic acid

OCA: Obeticholic acid

PKA: Protein kinase A

Rp-cAMPS: Competitive inhibitor of the activation of cAMP-dependent protein kinases by cAMP

TCDC: Taurochenodeoxycholic acid

TGR5: G protein-coupled bile acid receptor 1

TβMCA: Tauro β-Muricholic acid

TUDCA: Tauroursodeoxycholic acid

UDCA: Ursodeoxycholic acid

Acknowledgements

We thank M. Carlenossi, M. S. Ramon and M. L. Navarro for their expert technical assistance. This work was supported by grants from Fundacão de Amparo á Pesquisa do Estado de São Paulo (FAPESP 2013/01318-4), Conselho Nacional para o Desenvolvimento Científico e Tecnológico (CNPq 200030/2014-0), Instituto Nacional de Obesidade e Diabetes (CNPq/FAPESP) and Coordenação de Aperfeiçoamento de Pessoal de Nível Superior (CAPES). This study was also supported by grants from the Spanish Ministerio de Ciencia e Innovación (BFU2013-42789-P; BFU2011-28358). CIBERDEM is an initiative of the Instituto de Salud Carlos III.

Conflict of interest

All contributing authors report no conflict of interest.

ABSTRACT

Objective: While bile acids are important for the digestion process, they also act as signaling molecules in many tissues, including the endocrine pancreas, which expresses specific bile acid receptors that regulate several cell functions. In this study, we investigated the effects of the conjugated bile acid TUDCA on glucose-stimulated insulin secretion (GSIS) from pancreatic β-cells.

Methods: Pancreatic islets were isolated from 90-day-old male mice. Insulin secretion was measured by radioimmunoassay, protein phosphorylation by western blot, Ca^{2+} signals by fluorescence microscopy and ATP-dependent K^+ (K_{ATP}) channels by electrophysiology.

Results: TUDCA dose-dependently increased GSIS in fresh islets at stimulatory glucose concentrations but remained without effect at low glucose levels. This effect was not associated with changes in glucose metabolism, Ca^{2+} signals or K_{ATP} channel activity; however, it was lost in the presence of a cAMP competitor or a PKA inhibitor. Additionally, PKA and CREB phosphorylation were observed after 1-hour incubation with TUDCA. The potentiation of GSIS was blunted by the Gα stimulatory, G protein subunit-specific inhibitor NF449 and mimicked by the specific TGR5 agonist INT-777, pointing to the involvement of the bile acid G protein-coupled receptor TGR5.

Conclusion: Our data indicates that TUDCA potentiates GSIS through the cAMP/PKA pathway.

Keywords: β-cell, bile acids, insulin secretion, TUDCA

1. INTRODUCTION

Bile acids are molecules derived from cholesterol and synthesized in hepatocytes. They facilitate the digestion and absorption of dietary lipids and fat-soluble vitamins and regulate cholesterol excretion and sterol homeostasis. Before secretion into the gallbladder and duodenum, bile acids undergo a conjugation process with glycine or taurine, which increases their solubility and decreases the toxicity of these compounds [1, 2, 3]. In addition to the digestive function of bile acids, the discovery of bile acid receptors in the last couple of years has emphasized their role as extracellular messengers, which produce both genomic and non-genomic effects through multiple signaling pathways [1, 2, 4, 5]. Many tissues, including the endocrine pancreas, express bile acid receptors [6, 7]. The most important of these receptors are the nuclear receptor Farnesoid X Receptor (FXR) and the G protein-coupled bile acid receptor TGR5 [1, 2, 8].

The activation of FXR can regulate several processes in pancreatic β-cells. In the insulin-producing cell line βTC6, the FXR agonist 6-ethyl-chenodeoxycholic acid (6E-CDCA) increased the expression of insulin and the glucose-regulated transcription factor KLF11. It also induced AKT phosphorylation and GLUT-2 translocation to the plasma membrane, promoting glucose uptake [10]. The activation of FXR by the taurine-conjugated bile acid taurochenodeoxycholic acid (TCDC) increased glucose-stimulated insulin secretion (GSIS) in isolated mouse islets. This effect was associated with the inhibition of ATP-dependent K^+ (K_{ATP}) channels, changes in β-cell electrical activity, and increased Ca^{2+} influx [7]. The use of FXR ligands has also been explored in the treatment of glucose homeostasis disorders. The FXR ligand 6-ethyl-chenodeoxycholic acid (6E-CDCA) decreased glucose, triglyceride and cholesterol

112 levels in db/db mice and Zucker fa/fa rats, improving glucose homeostasis in these
113 diabetic models [8]. The FXR agonist obeticholic acid (OCA) ameliorated insulin
114 sensitivity and the metabolic profile in patients with type-2 diabetes [10]. Activation of
115 the G protein-coupled bile acid receptor TGR5 can also regulate pancreatic β-cell
116 function. The TGR5 ligands oleanolic acid (OA) and INT-777 stimulated GSIS in the
117 insulin-producing cells MIN-6 and human islets [6]. This effect depended on the
118 activation of the Gα stimulatory TGR5 subunit, increasing adenylyl cyclase activity,
119 cAMP levels, and cytosolic Ca^{2+} concentrations [6]. In rodents, synthetic TGR5 agonists
120 diminished plasma glucose and insulin levels and protected against high-fat diet-
121 induced obesity [11]. TGR5 was also shown to be involved in glucose homeostasis
122 through stimulation of the incretin glucagon-like peptide 1 (GLP-1) secretion [12, 13].

123 Although bile acids have recently been shown to be signaling messengers that
124 are able to regulate some cellular processes in the endocrine pancreas, there is little
125 information regarding their receptors, their molecular mechanisms and the actions
126 involved. In this study, we analyzed the effects of the taurine-conjugated bile acid
127 tauroursodeoxycholic acid (TUDCA) on the insulin secretory function of pancreatic β-
128 cells. TUDCA and ursodeoxycholic acid (UDCA) are used for the treatment of different
129 liver diseases, such as primary biliary cirrhosis and cholesterol gallstones, but they also
130 seem to have therapeutic potential in non-liver diseases, such as neurological, retinal,
131 metabolic and myocardial disorders [14, 15]. These effects seem to be associated with
132 their anti-apoptotic properties. Additionally, studies in experimental models of obesity
133 have reported that TUDCA can act as a chemical chaperone that ameliorates insulin
134 resistance by reducing endoplasmic reticulum stress and the unfolded protein response

135 [16]. Here, we show that TUDCA potentiates GSIS in pancreatic β-cells, likely through
136 the bile acid receptor TGR5 and activation of the cAMP/PKA pathway.

137

2. MATERIALS AND METHODS

2.1 Reagents. TUDCA was purchased from Calbiochem (São Paulo, SP, BRA, cat. 580549), and ^{125}I was purchased from Genesis (São Paulo, SP, BRA). Western Blot reagents were purchased from Bio-Rad (Madrid, Spain), and antibodies were purchased from Cell Signaling (Barcelona, Spain). The remaining reagents were purchased from Sigma Chemical (St. Louis, MO, USA).

2.2 Animals. All experiments involving animals were approved by the Animal Care Committee at UNICAMP (License Number: 2234-1) and Miguel Hernández University (ref. UMH.IB.IQM.01.13). Male 90-day-old C57Bl/6 mice were obtained from the breeding colony at UNICAMP and UMH and were maintained at 22 ± 1ºC on a 12-h light–dark cycle with free access to food and water. Mice were euthanized in a CO_2 chamber and decapitated for pancreatic islet isolation by collagenase digestion of the pancreas, as previous described [17].

2.3 Insulin secretion. For static insulin secretion, pancreatic islets (4 islets per well) were incubated for 30 min with Krebs-Bicarbonate buffer (KBB; (in mM) 115 NaCl, 5 KCl, 2.56 $CaCl_2$, 1 $MgCl_2$, 10 $NaHCO_3$, 15 HEPES), supplemented with 5.6 mM glucose and 0.3 % BSA and equilibrated with a mixture of 95 % O_2/5 % CO_2 to regulate the pH at 7.4. After 30 min of preincubation time, the medium was removed and immediately replaced with fresh KBB medium containing different glucose and TUDCA concentrations, as well as the different reagents indicated in the experiments. After 1 h of incubation time, the medium was removed and stored at –20°C. For islet insulin content, groups of four islets were collected and transferred to tubes containing 1 mL of deionized water, and the islet cells were homogenized using a sonicator

(Brinkmann Instruments, USA). Insulin levels were measured by a radioimmunoassay (RIA). Total islet protein was assayed using the Bradford dye method [18] with BSA as the standard curve.

2.4 Cytoplasmic Ca^{2+} oscillations and NAD(P)H fluorescence. For cytoplasmic Ca^{2+} oscillations, fresh isolated islets were incubated with fura-2 acetoxymethyl ester (5 µmol/L) for 1 hour at 37ºC in KBB buffer that contained 5.6 mM glucose, 0.3 % BSA and pH 7.4. Islets were then washed with the same medium and placed in a chamber that was thermostatically regulated at 37ºC on the stage of an inverted microscope (Nikon UK, Kingston, UK). Islets were perfused with albumin-free KBB that was continuously gassed with 95 % O_2/5 % CO_2 (pH 7.4). A ratio image was acquired every 5 s with an ORCA-100 CCD camera (Hammamatsu Photonics, Iberica, Barcelona, Spain) in conjunction with a Lambda-10-CS dual filter wheel (Sutter Instrument Company, CA, USA), which was equipped with 340 and 380 nm, 10 nm bandpass filters and a range of neutral density filters (Omega opticals, Stanmore, UK). Ca^{2+}-dependent fluorescence in the recordings was displayed as the ratio F_{340}/F_{380}. The analysis was obtained using ImageMaster3 software (Photon Technology International, NJ, USA) [19]. Some data were represented as the area under the curve (AUC) of the last 10 min of the stimuli as a measure of the global Ca^{2+} entry [20]. NAD(P)H fluorescence was monitored using the same above-mentioned system, but fresh islets were excited with a 365-nm band pass filter, and the emission was filtered at 445 ± 25 nm [21]. An image was acquired every 60 sec.

2.5 Western blot analysis. Groups of 250 isolated islets were incubated in KBB medium containing 11.1 mM glucose and 50 µM TUDCA. Islets were then homogenized with 9 µL of Cell Lysis Buffer (Cell Signaling Technology, Danvers,

MA) and incubated for 0, 10, 20, 30 and 60 min in the conditions indicated in the figure legends. For SDS gel electrophoresis and western blot analysis, the samples were treated with a Laemmli sample buffer containing dithiothreitol. After heating to 95ºC for 5 min, the proteins were separated by electrophoresis in a 4–20% Mini Protean Gel (Bio-Rad, Hercules, CA, USA). Prestained SDS-PAGE standards were included for molecular mass estimation. Transfer to PVDF membranes was performed in a Trans Blot Turbo transfer for 7 min at 25 V with TRIS/glycine buffer (Bio-Rad, Hercules, CA, USA). After the membranes were blocked with 5% non-fat dry milk buffer (5% milk, 10 mM TRIS, 150 mM NaCl and 0.02% Tween 20), they were incubated with a polyclonal antibody against phosphorylated (p)-CREB^{Ser133} (1:1000; Cell Signaling #9198), CREB (1:1000; Cell signaling #4820), pPKA C^{Thr197} (1:1000; Cell Signaling #5661), PKA C-α (1:1000; Cell signaling #4782) or GAPDH (1:1000; Cell Signaling #5174). GAPDH was used as a control for the experiment. The visualization of specific protein bands was performed by incubating the membranes with the appropriate secondary antibodies. Protein bands were revealed by using the Chemi Doc MP System (Bio-Rad, Hercules, CA, USA), which detects the chemiluminescence. The band intensities were quantified with Image Lab Lale 4.1 TM Software (Bio-Rad, Hercules, CA, USA).

2.6 Patch-clamp recordings

Islets were dispersed into single cells and cultured as previously described [22]. K_{ATP} channel activity was recorded using standard patch-clamp recording procedures. Currents were recorded by using an Axopatch 200B patch-clamp amplifier (Axon Instruments Inc., Union City, CA). Patch pipettes were pulled from borosilicate capillaries (Sutter Instrument Co., Novato, CA) using a flaming/brown micropipette

puller P-97 (Sutter Instrument Co.) with resistance between 3 and 5 MΩ when filled with pipette solutions, as specified below. The bath solution contained 5 mM KCl, 135 mM NaCl, 2.5 mM $CaCl_2$, 10 mM HEPES, and 1.1 mM $MgCl_2$ (pH 7.4), and it supplemented with glucose as indicated. The pipette solution contained 140 mM KCl, 1 mM $MgCl_2$, 10 mM HEPES and 1 mM EGTA (pH 7.2). The pipette potential was held at 0 mV throughout the recording process. K_{ATP} channel activity was quantified by digitizing 60 sec sections of the current record filtered at 1 kHz and sampled at 10 kHz by a Digidata 1322A (Axon Instruments Inc., Orleans Drive Sunnyvale, CA, USA) and calculating the mean *NPo* during the sweep. Channel activity was defined as the product of *N*, the number of functional channels, and *Po*, the open state probability. *Po* was determined by dividing the total time channels spent in the open state by the total sample time. Values of *NPo* were normalized relative to the channel activity measured in control conditions before the application of different substances. Data sampling was initiated 1 min before (control) and 10–15 min after the application of the test substances. Experiments were carried out at room temperature (20–24ºC). These experiments were performed at 8 mM glucose, since at 11.1 mM glucose concentrations the majority of K_{ATP} channels are closed [20, 21, 22].

2.7 Statistical analysis. The results are presented as the mean ± SEM for the number of determinations (n) indicated. Statistical analysis was performed using Student's t test or ANOVA with the appropriate post-test using Graph Pad Prism 5.0 software (La Jolla, CA, USA).

3. RESULTS

3.1 TUDCA stimulates insulin secretion in isolated islets. Mouse pancreatic islets incubated with TUDCA released more insulin than controls in a glucose-dependent manner. Although this bile acid had no effect at low concentrations, it increased glucose-induced insulin secretion (GSIS) at concentrations higher than 10 μM (Fig. 1). To address the mechanisms involved in the effects of TUDCA on GSIS, we performed the following experiments at a concentration of 50 μM. In agreement with the previous result, figure 2A shows that TUDCA increased insulin release from mouse islets incubated with 11 mM or higher glucose concentrations. The half-maximal effect (EC50) obtained from the dose-response curve (Fig. 2B) was calculated to be 13.78 ± 1.03 mM glucose in islets incubated with TUDCA versus 15.47 ± 0.63 mM in controls. As indicated by the shift to the left of the dose-response curve and the magnitude of the secretory responses, TUDCA increased the β-cell responsiveness to glucose, leading to enhanced GSIS. No differences were observed in the total insulin content between TUDCA-treated and control cells (Fig. 2C), indicating that changes in insulin release were not mediated by TUDCA effects on insulin synthesis.

3.2 TUDCA did not alter glucose-regulated NAD(P)H levels, electrical activity or Ca^{2+} signals in isolated islets. Several cell processes are involved in GSIS. When glucose enters β-cells, mitochondrial metabolism increases the cytosolic ATP/ADP ratio, leading to the closure of the K_{ATP} channels, which depolarizes the plasma membrane potential. This depolarization activates voltage-dependent Ca^{2+} channels, triggering a cytosolic Ca^{2+} rise that stimulates secretion. To study the involvement of these processes, we first monitored the glucose-induced changes through NAD(P)H levels. These levels increase as a result of glycolysis and Krebs cycle activation by

glucose, processes that are coupled to mitochondrial ATP production [23]. When mouse pancreatic islets were perfused in the presence or absence of the bile acid (Fig. 3A, B), no differences in glucose-induced NAD(P)H fluorescence levels were detected between the groups. We also explored the effect of TUDCA on glucose-regulated K_{ATP} channel activity because some bile acids, such as TCDC, have been shown to modulate this channel in pancreatic β-cells [7]. As shown in Figure 3C and D, TUDCA did not produce any effect on K_{ATP} channel activity with 8 mM glucose. These findings also indicate that TUDCA did not affect mitochondrial metabolism (as observed in Figure 3A and B) because the K_{ATP} channel is highly sensitive to alterations in mitochondrial function and ATP levels [24]. Diazoxide is a potent K_{ATP} channel opener, which hyperpolarizes the plasma membrane, leading to reduced intracellular Ca^{2+} levels and insulin secretion. As expected, diazoxide decreased insulin secretion induced by 11 mM glucose (Supplementary Fig. 2A). Despite the inhibitory effect of the K_{ATP} channel opener, TUDCA was able to increase insulin secretion in the presence of diazoxide, suggesting that TUDCA effects are likely mediated by an alternative pathway that differs from the K_{ATP} channel route. Finally, we analyzed the effect of TUDCA on glucose-induced Ca^{2+} signals. TUDCA did not generate any effect when it was acutely applied to mouse islets in basal conditions (Fig. 4A) or after the generation of a Ca^{2+} increase with 11 mM glucose (Fig. 4B). No differences were observed in response to 11.1, 16.7 or 22.2 mM glucose in pancreatic islets continuously perfused in the presence of 50 μM TUDCA compared to controls either (Fig. 4C–G and Supplementary. Fig. 1). Thus, it seems that the effect of TUDCA on GSIS is not mediated by K_{ATP} channel-dependent mechanisms or Ca^{2+} signals.

3.3 The effects of TUDCA on GSIS likely depend on the G protein-coupled bile acid receptor TGR5. To further investigate the role of TUDCA on intracellular pathways, we also explored the types of bile acid receptors that were involved. Given that TUDCA has poor affinity for the nuclear receptor FXR [2, 3], we focused on TGR5, which is a G protein-coupled receptor that couples to the Gα stimulatory subunit, leading to the activation of adenylyl cyclase, the generation of cAMP and, subsequently, the activation of PKA [1]. We used NF449, a specific inhibitor of the Gα stimulatory G protein subunit. This inhibitor did not alter GSIS at 11.1 or 22.2 mM glucose levels (Fig. 5A and B), yet it abolished the stimulatory effects of TUDCA on GSIS at both glucose concentrations. Because there are no commercially available TGR5-selective antagonists [25], we tested the effect of INT-777 (6-alpha-ethyl-23(*S*)-methyl-cholic acid, 6-EMCA), a potent and selective TGR5 agonist. INT-777 totally mimicked the TUDCA action of 11 mM glucose, whereas it had no effect at basal glucose concentrations (Fig. 5B). These results indicate that a G protein-coupled receptor mediates TUDCA actions, likely via the TGR5 bile acid receptor. We also analyzed the effects of tauro β-muricholic acid (TβMCA), a natural FXR antagonist, to analyze whether this receptor participates in the actions of TUDCA. Incubation with TβMCA did not alter the effect of TUDCA on insulin secretion, indicating that this FXR was not involved (Supplementary Fig. 2B).

3.4 TUDCA-stimulated insulin secretion is dependent on the cAMP/PKA pathway. To address whether the cAMP/PKA pathway could be modulated by TUDCA, we investigated the effect of the PKA inhibitor H89 and (Rp)-cAMP, a competitive inhibitor of PKA activation by cAMP, on GSIS. In both cases, the inhibition of the PKA pathway completely blunted the TUDCA actions on GSIS from mouse pancreatic islet

302 cells (Fig. 6A and B). In addition, to confirm the activation of this pathway, we
303 analyzed the phosphorylation levels of PKA and its target protein CREB in a time-
304 dependent manner (Fig. 6C and D). TUDCA enhanced PKA and CREB
305 phosphorylation after being incubated for 20 min. In addition, enhanced pPKA content
306 was also observed after 1 h.

307

4. DISCUSSION

The present study shows that the taurine-conjugated bile acid TUDCA has a positive effect on glucose-induced insulin secretion from mouse isolated pancreatic islets, whereas it remains without effect at basal glucose levels. This behavior is similar to that of incretins such as GLP-1. Incretins exhibit an important therapeutic advantage for glycemic control in diabetes because they act on hyperglycemic conditions without favoring hypoglycemic episodes [26]. Thus, glucose-dependent TUDCA action on insulin secretion might be interesting from a therapeutic context. Currently, TUDCA and ursodeoxycholic acid (UDCA) are used for the treatment of several liver diseases [14,15]. In contrast to other bile acids, which are cytotoxic, TUDCA and UDCA exhibit protective properties against apoptosis [27]. Additionally, ongoing research is analyzing the therapeutic potential of TUDCA to alleviate apoptosis in non-liver diseases, such as neurological, retinal, metabolic and myocardial disorders [14, 15]. It has been reported in obese humans and mice that TUDCA ameliorates insulin resistance by reducing endoplasmic reticulum stress [6]. In addition to all of these beneficial properties, here, we show that TUDCA potentiates GSIS via bile acid signaling involving the cAMP/PKA pathway. This effect occurred over a short time period (less than 1 h) and was not mediated by genomic actions because insulin protein synthesis remained unchanged (Fig. 1 and 2). It remains to be explored whether in vitro TUDCA effects on GSIS are also important for in vivo conditions to acutely modulate plasma insulin levels and glucose homeostasis. It would also be interesting to analyze whether in vivo treatment with TUDCA alone or in combination with other therapeutic agents could ameliorate glycemic values in animal models of obesity and diabetes.

Although FXR and TGR5 are both expressed in mouse pancreatic islets [6, 7, 9], several findings support that the effects of TUDCA observed in this study were mediated, at least in part, by TGR5. In contrast to the nuclear FXR receptor, TGR5 is a plasma membrane receptor that is coupled to a G protein (Gα stimulatory), which activates adenylate cyclase, increasing cAMP levels. This results in PKA activation, inducing CREB phosphorylation [2, 3, 28]. Our results showed that the effects of TUDCA on GSIS were blocked when we inhibited both a G protein (Gα stimulatory) and PKA (Fig. 5 and 6). Additionally, TUDCA actions were mimicked by a TGR5 selective agonist. We also showed that TUDCA increases PKA and CREB phosphorylation levels on the same temporal scale as the effects on GSIS. Remarkably, although TUDCA has been reported to activate TGR5 and to induce cAMP production [29, 30], this hydrophilic bile acid and UDCA are not FXR agonists [2, 30] because the latter receptor exhibits more affinity for hydrophobic bile acids. Taurine conjugation of UDCA may also increase its affinity for TGR5 [25, 31]. In contrast to the effects of the FXR agonist TCDC reported in mouse pancreatic islets [7], TUDCA actions on GSIS were independent of K_{ATP} channels and changes to cytosolic Ca^{2+} levels. These findings further support the idea that TUDCA affected secretion in the current study by mechanisms other than FXR activation.

Short-term non-genomic effects on insulin secretion by some bile acids have been previously reported. The conjugated bile acid TCDC induced insulin release at high glucose concentrations via FXR activation in mouse β-cells [7]. In MIN-6 cells and human islets, the TGR5 agonists oleanolic (OA) and lithocholic acid (LCA) stimulated insulin secretion in both basal and stimulatory glucose conditions [6]. TUDCA enhanced insulin secretion in pig pancreatic islets at high glucose concentrations [32].

In the latter study, the bile acid receptor mediating these TUDCA effects was not explored. Our findings are in agreement with these studies, showing that TUDCA stimulates high glucose-induced insulin secretion in the short-term. In βTC6 cells and human islets, the FXR ligand 6E-CDCA [9] was reported to enhance GSIS after an 18 h incubation. However, genomic actions were likely involved at these long periods because this FXR ligand also induced insulin expression.

It has been shown that bile acids can regulate the activity of plasma membrane ion channels and cytosolic Ca^{2+} signals in different cell types [31]. In mouse isolated islets, the FXR agonist TCDC leads to the blockade of K_{ATP} channel currents, stimulating electrical activity and intracellular Ca^{2+} oscillations [7]. In MIN6 cells, mouse islets and human islets, different TGR5 agonists generate a rise in intracellular Ca^{2+} [6]. In this latter work, TGR5 activation led to phosphoinositide hydrolysis and Ca^{2+} release from intracellular stores. In our study, we did not observe any effects of TUDCA on K_{ATP} channel activity (Fig. 3), Ca^{2+} signals or intracellular Ca^{2+} release (Fig. 4), indicating that these pathways were not involved. It has been shown that the pharmacological activation of PKA can slightly increase glucose-induced intracellular Ca^{2+} concentrations [33]. Because we did not observe any effect on cytosolic Ca^{2+} levels, it seems that TUDCA may induce PKA activation to a low extent (at least compared with a pharmacological agonist) or that PKA-induced activation by TUDCA preferentially affects the secretory process. Indeed, changes in cAMP levels close to the plasma membrane and spatial compartmentalization of several components of the exocytotic process seem to play a major role in GSIS in pancreatic β-cells [34].

TGR5 is a G protein-coupled receptor that leads to adenylate cyclase activation [31]. In the present study, incubation of isolated fresh islets with NF449, a Gαs subunit

inhibitor, prevented the effects of TUDCA on GSIS. Likewise, the inhibition of PKA activity with H89 or Rp-cAMPS resulted in the blockade of TUDCA actions. Finally, TUDCA led to PKA phosphorylation and activation of its target CREB in isolated mouse islets in the short-term. All of these findings indicate that the effects of TUDCA on GSIS are cAMP/PKA-dependent. The role of the cAMP/adenylate cyclase pathway in GSIS is well known. Elevation of cAMP concentrations potentiates glucose-dependent insulin secretion through the activation of PKA [33, 35]. PKA phosphorylation affects the regulation of some proteins involved in exocytosis, thus stimulating insulin secretion in pancreatic β-cells [35, 36]. The present results are in agreement with previous studies on enteroendocrine cells showing that TGR5 activation is followed by Gαs release and activation of adenylate cyclase, leading to an increase in cAMP concentration and activation of PKA and CREB [3].

In summary, this study shows an important effect of TUDCA in mouse pancreatic β-cells. This bile acid increases insulin secretion only at high glucose concentrations by a mechanism that is mediated by the cAMP/PKA/CREB pathway. Although our experiments indicate that the TGR5 receptor is likely involved in the effects of TUDCA, we cannot rule out the implication of the FXR receptor and other signaling pathways.

Author contributions

J.F.V., R.A.R., I.Q., E.M.C., A.C.B., and A.N. designed the study, researched data, and wrote the paper. P.C.B., R.C.S.B., B.M., and S.S. researched data. R.A.R., E.M.C., I.Q., and J.F.V. contributed to the discussion and reviewed and edited the manuscript. J.F.V.

403 is the guarantor of this work and with full access to all of the data in the study and takes
404 responsibility for it.
405
406
407
408

5. REFERENCES

[1] Bunnett N. W., Neuro-humoral signalling by bile acids and the TGR5 receptor in the gastrointestinal tract. J Physiol. 2014, 592, 2943-50.

[2] Chiang J. Y. L., Bile Acid Metabolism and Signaling. Comprehensive Physiology. 2013, 3.

[3] Thomas C., Pellicciari R., Pruzanski M., Auwerx J., Schoonjans K., Targeting bile-acid signalling for metabolic diseases. Nat Rev Drug Discov. 2008, 7(8), 678-93.

[4] Nakajima T. Y., Okuda, K., Chisaki, W., S., Shin K., et al., Bile acids increase intracellular Ca(2+) concentration and nitric oxide production in vascular endothelial cells. Br J Pharmacol, 200, 130, 1457-67.

[5] Fu D., Wakabayashi Y., Lippincott-Schwartz J., Arias I., M., Bile acid stimulates hepatocyte polarization through a cAMP-Epac-MEK-LKB1-AMPK pathway. Proc Natl Acad Sci. 2011, 108, 1403-8.

[6] Kumar D., P., Rajagopal S., Mahavadi S., Mirshahi F., et al., Activation of transmembrane bile acid receptor TGR5 stimulates insulin secretion in pancreatic β cells. Biochem Biophys Res Commun. 2012, 427, 600-5.

[7] Düfer M., Hörth K., Wagner R., Schittenhelm B., et al., Bile acids acutely stimulate insulin secretion of mouse β-cells via farnesoid X receptor activation and K(ATP) channel inhibition. Diabetes. 2012, 61, 1479-89.

[8] Cipriani S., Mencarelli A., Palladino G., Fiorucci S., FXR activation reverses insulin resistance and lipid abnormalities and protects against liver steatosis in Zucker (fa/fa) obese rats. J Lipid Res. 2010, 51, 771-84.

[9] Renga B., Mencarelli A., Vavassori P., Brancaleone V., Fiorucci S., The bile acid sensor FXR regulates insulin transcription and secretion. Biochim Biophys Acta. 2010, 1802, 363-72.

[10] Mudaliar S., Henry R., R., Sanyal A., J., Morrow L., et al., Efficacy and safety of the farnesoid X receptor agonist obeticholic acid in patients with type 2 diabetes and nonalcoholic fatty liver disease. Gastroenterology. 2013, 145, 574-82

437 [11] Sato H., Genet C., Strehle A., Thomas C., et al., Anti-hyperglycemic activity of
438 a TGR5 agonist isolated from Olea europaea. Biochem Biophys Res Commun .2007,
439 362-793.

440 [12] Katsuma S., Hirasawa A., Tsujimoto G., Bile acids promote glucagon-like
441 peptide-1 secretion through TGR5 in a murine enteroendocrine cell line STC-1.
442 Biochem Biophys Res Commun. 2005, 329, 386-90.

443 [13] Bala V., Rajagopal S., Kumar D., P., Nalli A., D., et al., Release of GLP-1 and
444 PYY in response to the activation of G protein-coupled bile acid receptor TGR5 is
445 mediated by Epac/PLC pathway and modulated by endogenous H2S. Front Physiol.
446 2014, 3, 420.

447 [14] Vang S., Longley K., Steer C., J., Low W., C., The Unexpected Uses of Urso-
448 and Tauroursodeoxycholic Acid in the Treatment of Non-liver Diseases. Glob Adv
449 Health Med. 2014, 3, 58-69.

450 [15] Amaral J., D., Viana R., J., Ramalho R., M., Steer C., J., Rodrigues C., M., Bile
451 acids: regulation of apoptosis by ursodeoxycholic acid. J Lipid Res. 2009, 50, 1721-34.

452 [16] Ozcan U., Yilmaz E., Ozcan L., Furuhashi M., et al., Chemical chaperones
453 reduce ER stress and restore glucose homeostasis in a mouse model of type 2 diabetes.
454 Science. 2006,313, 1137-40.

455 [17] Bordin S., Boschero A., C., Carneiro E., M., Atwater I., Ionic mechanisms
456 involved in the regulation of insulin secretion by muscarinic agonists.J Membr Biol.
457 1995, 148, 177-84.

458 [18] Bradford M., M., A rapid and sensitive method for the quantitation of
459 microgram quantities of protein utilizing the principle of protein-dye binding. Anal
460 Biochem. 1976, 72, 248-54.

461 [19] Carneiro E., M., Latorraca M., Q., Araujo E., Beltrá M., et al., Taurine
462 supplementation modulates glucose homeostasis and islet function. J Nutr Biochem.
463 2009, 7, 503-11.

[20] Soriano S., Gonzalez A., Marroquí L., Tudurí E., Reduced insulin secretion in protein malnourished mice is associated with multiple changes in the beta-cell stimulus-secretion coupling. Endocrinology. 2010, 151, 3543-54.

[21] Rafacho A., Marroquí L., Taboga S., R., Abrantes J., L., et al., Glucocorticoids in vivo induce both insulin hypersecretion and enhanced glucose sensitivity of stimulus-secretion coupling in isolated rat islets. Endocrinology. 2010, 151, 85-95.

[22] Valdeolmillos M., Nadal A., Contreras D., Soria B., The relationship between glucose-induced K_ATP channel closure and the rise in [Ca2+]i in single mouse pancreatic β--cells. J Physiol . 1992, 455, 173-186.

[23] Eto K., Tsubamoto Y., Terauchi Y., Sugiyama T., et al., Role of NADH shuttle system in glucose-induced activation of mitochondrial metabolism and insulin secretion., Science. 1999, 283, 981-5.

[24] Carrasco A., J., Dzeja P., P., Alekseev A., E., Pucar D., et al., Adenylate kinase phosphotransfer communicates cellular energetic signals to ATP-sensitive potassium channels.Proc Natl Acad Sci. 2001, 98, 7623-8.

[25] Duboc H., Taché Y., Hofmann A., F., The bile acid TGR5 membrane receptor: from basic research to clinical application. Dig Liver Dis. 2014, 46, 302-12.

[26] Perfetti R., Merkel P., Glucagon-like peptide-1: a major regulator of pancreatic β-cell function. Eur J Endocrinol. 2000, 143, 717-25.

[27] Schoemaker M., H., Conde de la Rosa L., Buist-Homan M., Vrenken T., E., et al., Tauroursodeoxycholic acid protects rat hepatocytes from bile acid-induced apoptosis via activation of survival pathways. Hepatology. 2004, 39, 1563-73.

[28] Pols T., W., Noriega L., G., Nomura M., Auwerx J., et al., The bile acid membrane receptor TGR5: a valuable metabolic target. Dig Dis. 2011, 29, 37-44.

[29] Iguchi Y., Nishimaki-Mogami T., Yamaguchi M., Teraoka F., et al., Effects of chemical modification of ursodeoxycholic acid on TGR5 activation. Biol Pharm Bull. 2011, 34, 1-7.

[30] Sepe V., Renga B., Festa C., D'Amore C., et al., Modification on ursodeoxycholic acid (UDCA) scaffold and discovery of bile acid derivatives as selective agonists of cell-surface G-protein coupled bile acid receptor 1 (GP-BAR1). J Med Chem. 2014, 57, 7687-701.

[31] de Aguiar Vallim T., Q., Tarling E., J., Edwards P., A., Pleiotropic roles of bile acids in metabolism. Cell Metab. 2013, 17, 657-69.

[32] Lee Y., Y., Hong S., H., Lee Y., J., Chung S., S., et al., Tauroursodeoxycholate (TUDCA), chemical chaperone, enhances function of islets by reducing ER stress. Biochem Biophys Res Commun. 2010, 397, 735-9.

[33] Henquin J., C., Nenquin M., Activators of PKA and Epac distinctly influence insulin secretion and cytosolic Ca2+ in female mouse islets stimulated by glucose and tolbutamide. Endocrinology. 2014, 155, 3274-87.

[34] Idevall-Hagren O., Jakobsson I., Xu Y., Tengholm A., Spatial control of Epac2 activity by cAMP and Ca2+-mediated activation of Ras in pancreatic β cells. Sci Signal. 2013, 30, 273.

[35] Shibasaki T., Takahashi T., Takahashi H., Seino S., Cooperation between cAMP signalling and sulfonylurea in insulin secretion. Diabetes Obes Metab. 2014, 16 , 118-25.

[36] Song W., J, Seshadri M., Ashraf U., et al., Snapin mediates incretin action and augments glucose-dependent insulin secretion. Cell Metab. 2011, 13, 308–319.

518 **FIGURE LEGENDS**

519 **Figure 1: Effects of different TUDCA concentrations on glucose-induced insulin**
520 **secretion from mouse fresh islets.** Groups of 4 islets were incubated for 1 h with 2.8,
521 11.1, or 22.2 mM glucose (G) in the presence or absence of different TUDCA
522 concentrations. Data are displayed as the mean ± SEM of 10-15 islet groups. In all of
523 the experiments, glucose-induced secretion at 11.1 and 22.2 mM G was found to be
524 significantly higher compared to that of the basal condition (2.8 mM G). ***** and #,
525 significant differences ($p<0.05$) compared to the control conditions of 11.1 or 22.2 mM
526 G, respectively.

527

528 **Figure 2: The effect of TUDCA is glucose-dependent.** Effects of 50 µM TUDCA on
529 glucose-induced insulin secretion (A, B) and total insulin content (C) from fresh mouse
530 islets. Groups of 4 islets were incubated for 1 h at different glucose concentrations in
531 the presence or absence of 50 µM TUDCA (A). EC_{50} values are also displayed in (B).
532 Data are displayed as the mean ± SEM and were obtained from 10-15 groups of islets
533 for each glucose concentration. *****, significant differences ($p<0.05$) compared to control
534 conditions.

535

536 **Figure 3: TUDCA effects are not mediated by metabolic changes.** (A)
537 Representative records of the changes in NAD(P)H fluorescence (%) in response to 0.5,
538 5.6, 11.1 or 22.2 mM glucose from fresh mouse islets in the presence or absence of
539 TUDCA. (B) Increment in NAD(P)H fluorescence (%) for each glucose concentration.
540 Data are the mean ± SEM obtained from 4 to 6 independent experiments. (C, D)

Regulation of K_{ATP} channel activity in pancreatic β-cells of mice by 50 µM TUDCA. TUDCA did not produce any effect on the K_{ATP} channel activity at 8 mM glucose. (C) Records of K_{ATP} channel activity in the absence of glucose, 10 min after the application of 8 mM glucose, 10 min after the application of 8 mM glucose with 50 µM TUDCA, and 5 min after the application of 100 µM diazoxide. (D) Percentage of the K_{ATP} channel activity channel elicited by 0 mM glucose, 8 mM glucose, and 8 mM glucose and 50 µM TUDCA in single β-cells (n=6 cells). **, $p<0.01$ Student's t-test comparing 8 mM glucose and 8 mM glucose + 50 µM TUDCA with 0 mM glucose.

Figure 4: TUDCA does not affect glucose-induced Ca^{2+} signals. (A, B) Representative Ca^{2+} recordings from isolated islets showing the lack of TUDCA effects when acutely applied at basal (2.8 mM) and stimulatory (11.1 mM) glucose concentrations. Three independent experiments were performed for each condition. (C, D) Representative Ca^{2+} recordings in response to 11.1 or 16.7 mM glucose from fresh mouse islets. The experiments were performed in a perfusion system in the continuous presence or absence of 50 µM TUDCA. The AUC (E, F, G) of Ca^{2+} is displayed as an indicator of the global Ca^{2+} entry for the different glucose concentrations. Data are shown as the mean ± SEM and were obtained from 4 to 6 independent experiments.

Figure 5: TUDCA effects on GSIS are mediated by a G protein-coupled receptor. (A) TUDCA effects on insulin secretion induced by 11.1 and 22.2 mM glucose from mouse islets were abolished by the Gα stimulatory G protein subunit specific inhibitor NF449. (B) TUDCA effects on insulin secretion induced by 11.1 mM glucose from mouse islets were mimicked by the specific TGR5 agonist INT-777. Groups of 4 islets

were used in each measurement. Data are presented as the mean ± SEM and were obtained from 10 to 12 islets groups. *****, significant differences ($p<0.05$) compared to control conditions.

Figure 6: TUDCA actions on GSIS are mediated by the cAMP/PKA pathway. (A, B) Effects of TUDCA on GSIS from mouse islets after 1 h were blunted by the PKA inhibitor H89 (A) or by Rp-cAMP, a competitive inhibitor of PKA activation by cAMP (B). (C, D) TUDCA incubation for 1 h increases the phosphorylation of PKA (C) and CREB (D). Groups of 4 islets were used for insulin secretion measurements, and groups of 250 islets were used in the western blot experiments. Data are shown as the mean ± SEM and were obtained from 10 to 12 groups of islets. *****, significant differences ($p<0.05$) compared to control conditions.

Supplementary Figure 1: TUDCA does not affect glucose-induced Ca^{2+} signals. (A, B) Representative Ca^{2+} recordings from isolated islets showing the effect of TUDCA at basal (2.8 mM) and stimulatory (22.2 mM) glucose concentrations. Three independent experiments were performed in each condition. (C–H). The amplitude and Ca^{2+} oscillations from 22.2 and all of the glucose concentrations from the experiments shown in Figure 4. The experiments were performed in a perfusion system in the continuous presence or absence of 50 μM TUDCA. Data are shown as the mean ± SEM and were obtained from 4 to 6 independent experiments.

Supplementary Figure 2: TUDCA effects on glucose-stimulated insulin secretion (GSIS) are not mediated by a K_{ATP}-dependent mechanism and FXR receptor. (A)

587 TUDCA effects on insulin secretion induced by 11.1 mM glucose from mouse islets
588 were partially abolished by diazoxide. (B) TUDCA effects on insulin secretion induced
589 by 11.1 mM glucose from mouse islets were not abolished by the natural FXR inhibitor
590 TβMCA. Groups of 4 islets were used in each measurement. Data are displayed as the
591 mean ± SEM and were obtained from 6 to 8 islets groups. * and #, significant
592 differences ($p<0.05$) compared to control or control + DZX conditions, respectively.

Figure 01

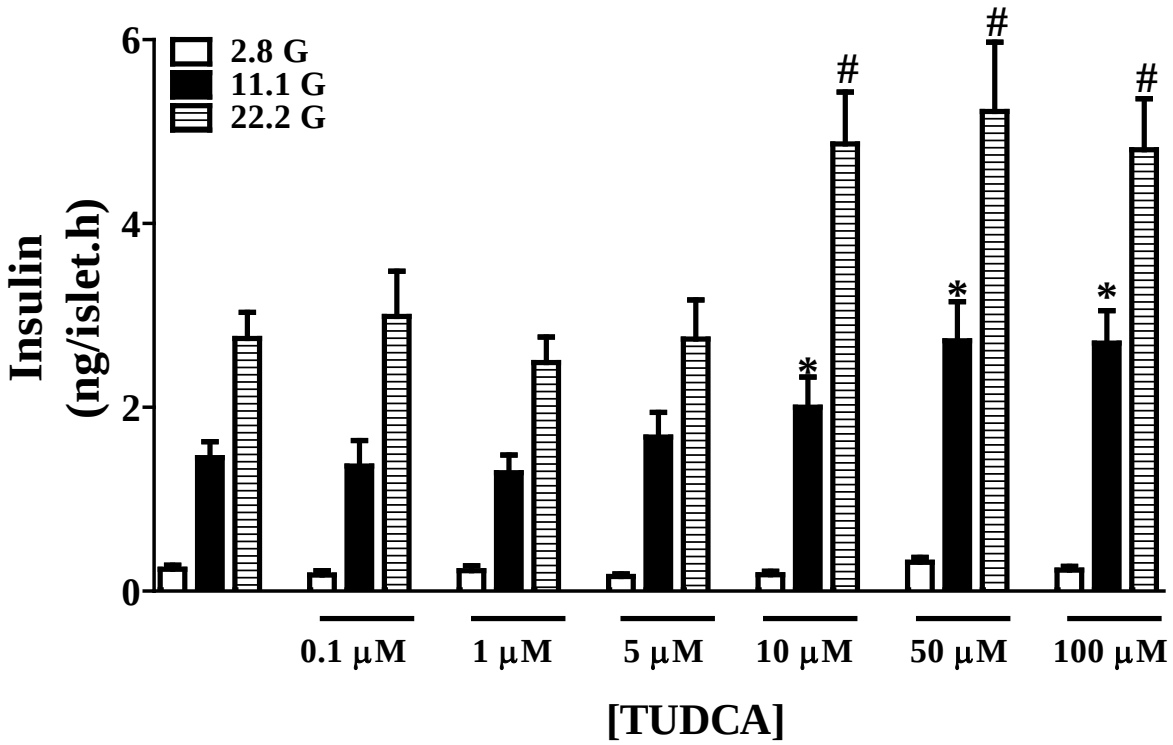
2.8 G
11.1 G
22.2 G
Insulin
(ng/islet.h)
6
4
2
0
#
#
#
*
*
*
0.1 μM
1 μM
5 μM
10 μM
50 μM
100 μM
[TUDCA]

Figure 02

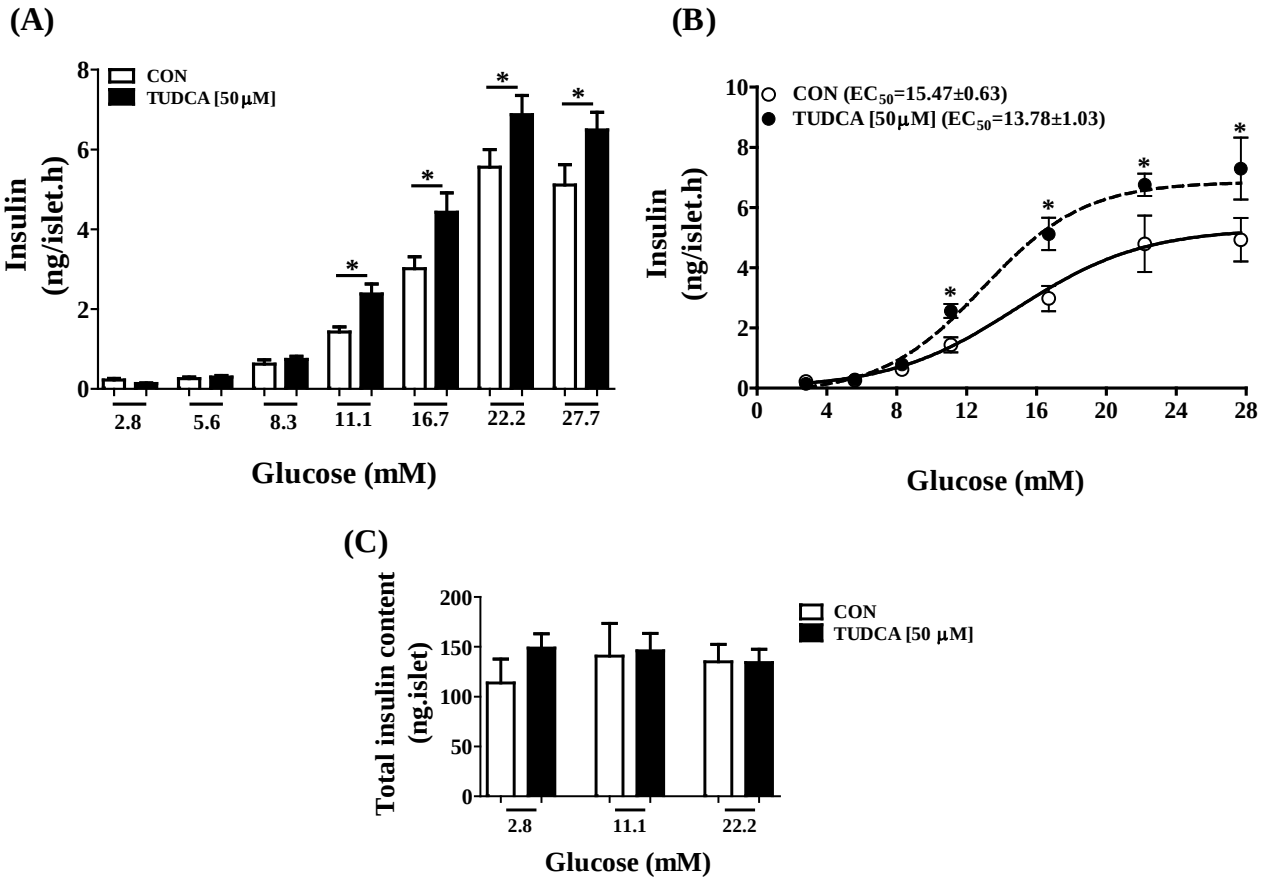
(A)
CON
TUDCA [50 μM]
Insulin (ng/islet.h)
0
2
4
6
8
2.8
5.6
8.3
11.1
16.7
22.2
27.7
Glucose (mM)
(B)
CON (EC50=15.47±0.63)
TUDCA [50μM] (EC50=13.78±1.03)
Insulin (ng/islet.h)
0
2
4
6
8
10
0
4
8
12
16
20
24
28
Glucose (mM)
(C)
Total insulin content (ng.islet)
0
50
100
150
200
CON
TUDCA [50 μM]
2.8
11.1
22.2
Glucose (mM)

Figure 03

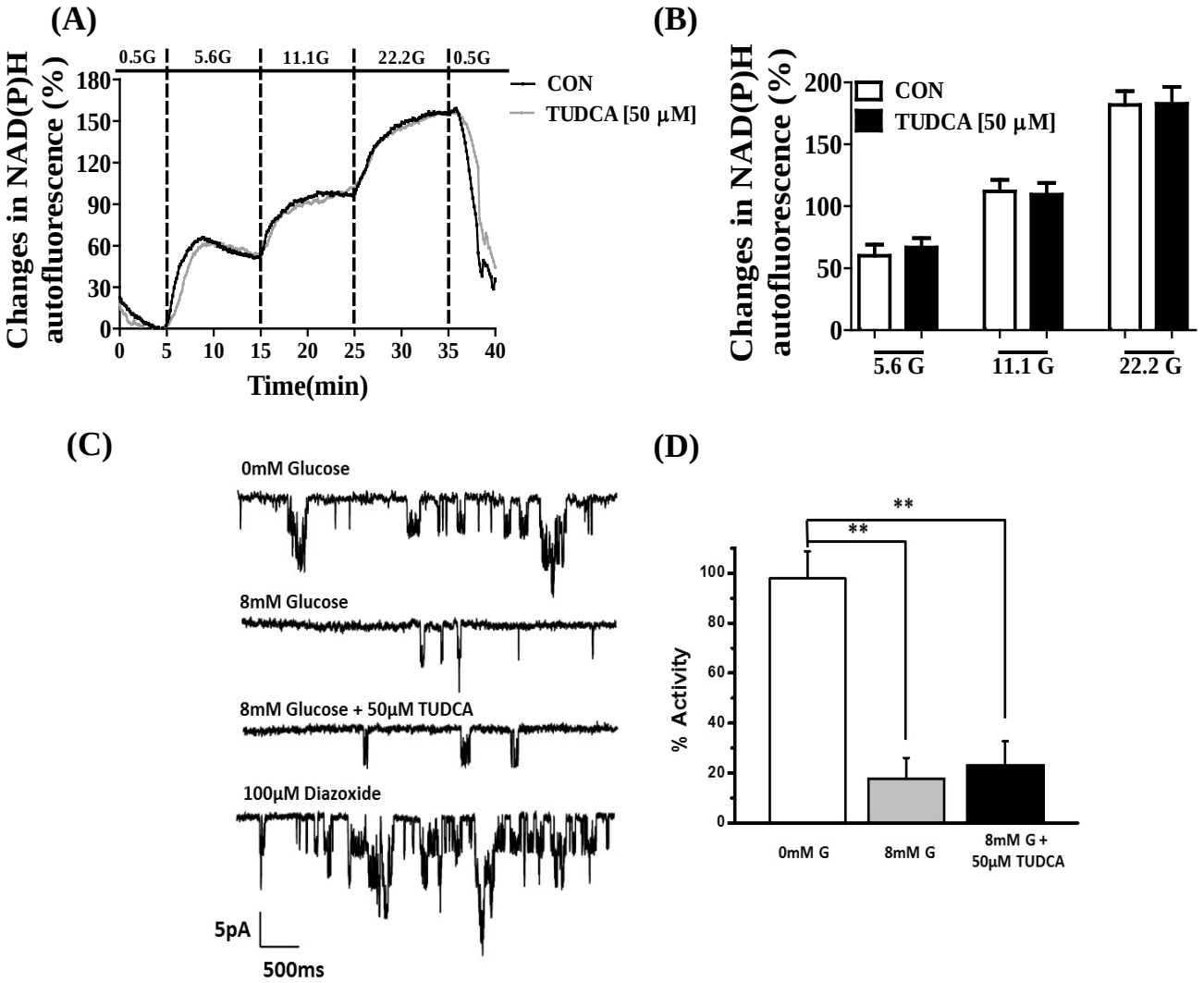
(A)
0.5G
5.6G
11.1G
22.2G
0.5G
CON
TUDCA [50 μM]
Changes in NAD(P)H autofluorescence (%)
Time(min)
(B)
CON
TUDCA [50 μM]
Changes in NAD(P)H autofluorescence (%)
5.6 G
11.1 G
22.2 G
(C)
0mM Glucose
8mM Glucose
8mM Glucose + 50μM TUDCA
100μM Diazoxide
5pA
500ms
(D)
% Activity
0mM G
8mM G
8mM G + 50μM TUDCA

Figure 04

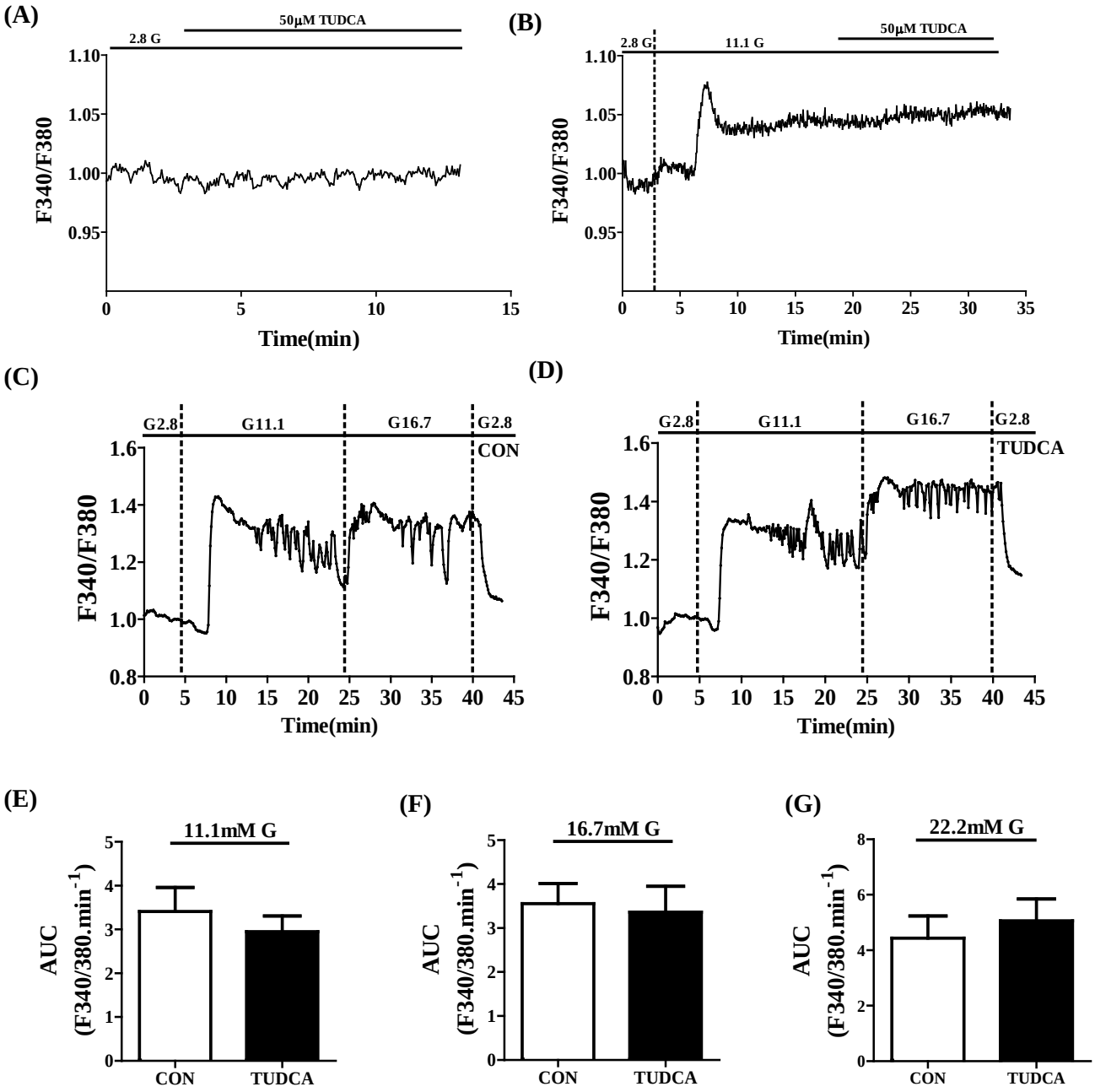
(A)
50μM TUDCA
2.8 G
F340/F380
Time(min)
(B)
2.8 G
11.1 G
50μM TUDCA
F340/F380
Time(min)
(C)
G2.8
G11.1
G16.7
G2.8
CON
F340/F380
Time(min)
(D)
G2.8
G11.1
G16.7
G2.8
TUDCA
F340/F380
Time(min)
(E)
11.1mM G
AUC
(F340/380.min-1)
CON
TUDCA
(F)
16.7mM G
AUC
(F340/380.min-1)
CON
TUDCA
(G)
22.2mM G
AUC
(F340/380.min-1)
CON
TUDCA

Figure 05

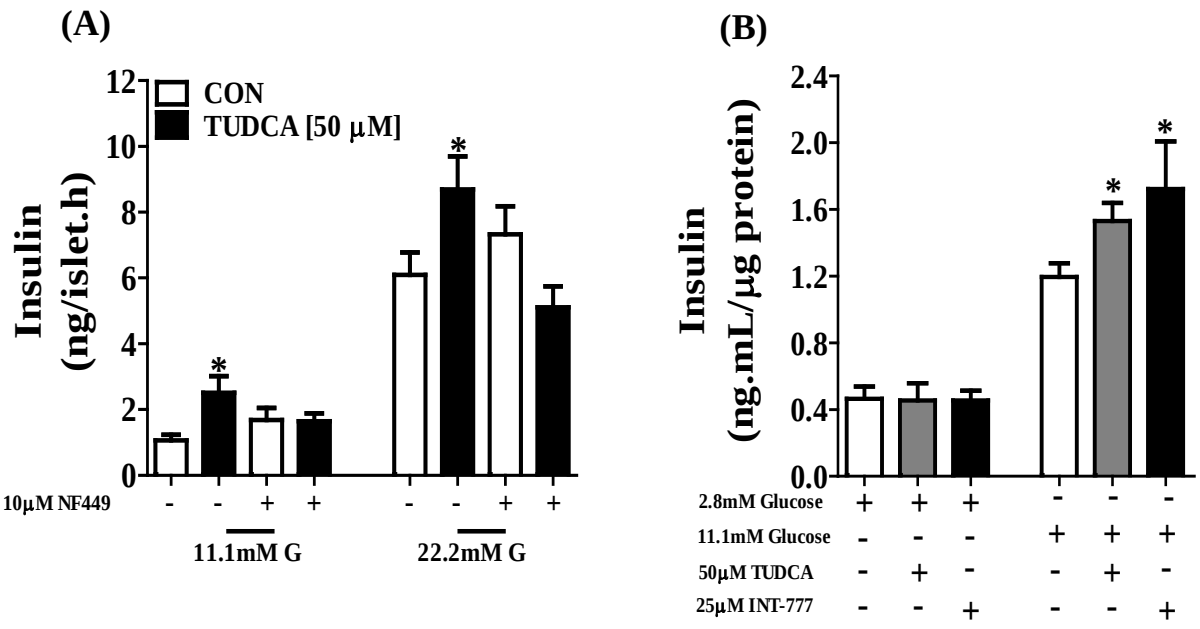
(A)
CON
TUDCA [50 μM]
Insulin (ng/islet.h)
12
10
8
6
4
2
0
*
*
10μM NF449 - - + + - - + +
11.1mM G
22.2mM G
(B)
Insulin (ng.mL/μg protein)
2.4
2.0
1.6
1.2
0.8
0.4
0.0
*
*
2.8mM Glucose + + + - - -
11.1mM Glucose - - - + + +
50μM TUDCA - + - - + -
25μM INT-777 - - + - - +

Figure 06

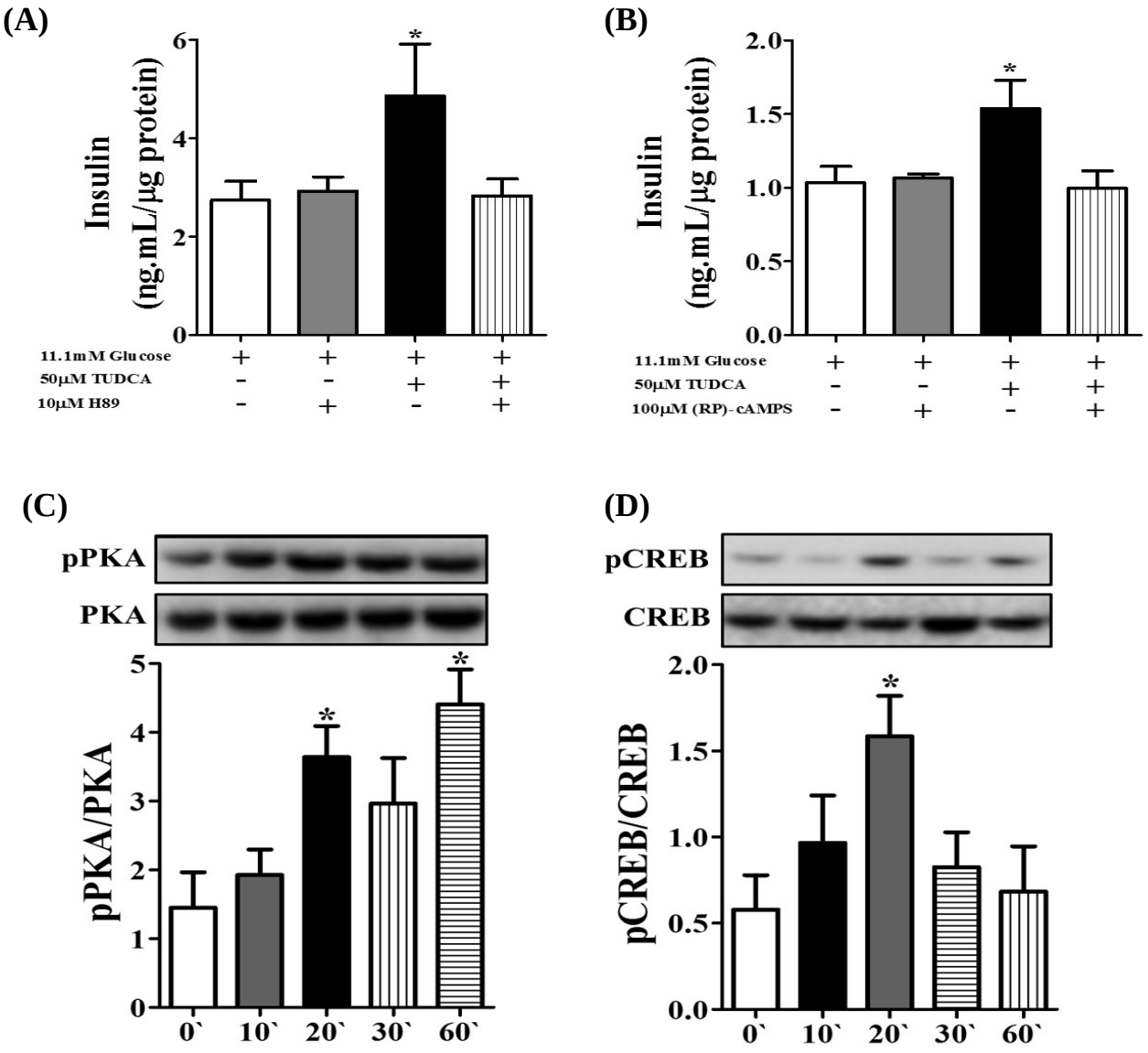
(A)
Insulin (ng.mL/μg protein)
6
4
2
0
*
11.1mM Glucose + + + +
50μM TUDCA - - + +
10μM H89 - + - +
(B)
Insulin (ng.mL/μg protein)
2.0
1.5
1.0
0.5
0.0
*
11.1mM Glucose + + + +
50μM TUDCA - - + +
100μM (RP)-cAMPS - + - +
(C)
pPKA
PKA
pPKA/PKA
5
4
3
2
1
0
* *
0` 10` 20` 30` 60`
(D)
pCREB
CREB
pCREB/CREB
2.0
1.5
1.0
0.5
0.0
*
0` 10` 20` 30` 60`

Supplementary 01

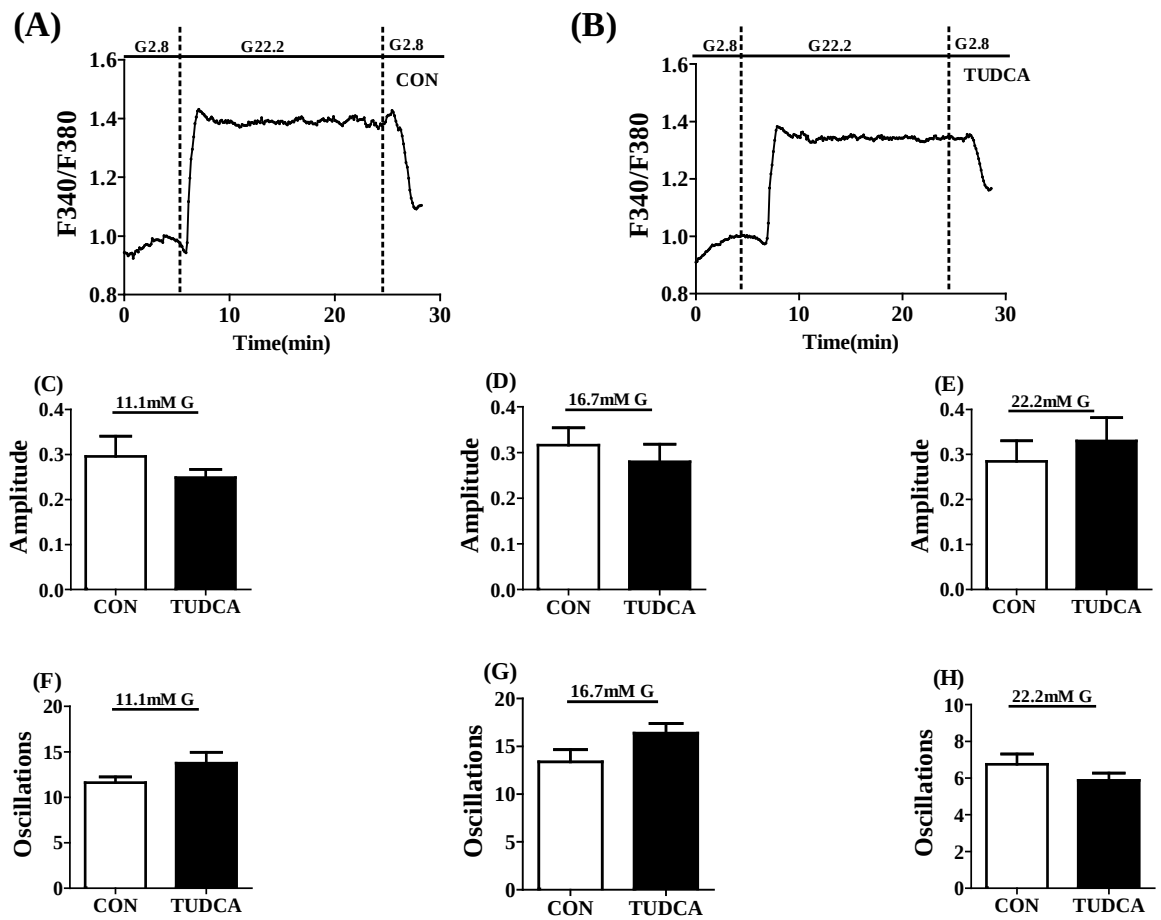

Supplementary 02